Bayona, V., Moscoso, M. & Kindelan, M. (2012). Optimal variable shape parameter for multiquadric based RBF-FD method. *Journal of Computational Physics*, 231(6), 2466-2481.

DOI: 10.1016/j.jcp.2011.11.036

Optimal variable shape parameter for multiquadric based RBF-FD method

Victor Bayona, Miguel Moscoso, and Manuel Kindelan

Gregorio Millán Institute, Universidad Carlos III de Madrid, Avenida de la Universidad 30, 28911 Leganés, Spain

Abstract

In this follow up paper to our previous study in [2], we present a new technique to compute the solution of PDEs with the multiquadric based RBF nite di erence method (RBF-FD) using an optimal node dependent variable value of the shape parameter. This optimal value is chosen so that, to leading order, the local approximation error of the RBF-FD formulas is zero. In our previous paper [2] we considered the case of an optimal (constant) value of the shape parameter for all the nodes. Our new results show that, if one allows the shape parameter to be di erent at each grid point of the domain, one may obtain very signi cant accuracy improvements with a simple and inexpensive numerical technique. We analyze the same examples studied in [2], both with structured and unstructured grids, and compare our new results with those obtained previously. We also nd that, if there are a signi cant number of nodes for which no optimal value of the shape parameter exists, then the improvement in accuracy deteriorates signi cantly. In those cases, we use generalized multiquadrics as RBFs and choose the exponent of the multiquadric at each node to assure the existence of an optimal variable shape parameter.

Key words: Radial basis functions; multiquadric; mesh-free; shape parameter

1 Introduction

The global RBF (Radial Basis Function) method was rst proposed by Edward Kansa [13,14] as a truly meshless method for the solution of partial di erential

Corresponding author. Address: Universidad Carlos III de Madrid, Avenida de la Universidad 30, 28911 Leganes, Spain. Fax: +34 91 624 91 29

Email addresses: vbayona@ing.uc3m.es (Victor Bayona), moscoso@math.uc3m.es (Miguel Moscoso), kinde@ing.uc3m.es (Manuel Kindelan).

equations (PDEs) on irregular domains. It is based on collocation of RBFs on a set of scattered nodes.

To overcome some of the drawbacks of the global RBF method, a local RBF method was independently proposed by several authors [24,26,28]. The method works very much like the nite di erence (FD) method: di erential operators at a given node are approximated as a weighted sum of the values of the sought function at some surrounding nodes. However, while in the FD method the unknown weights are computed using polynomial interpolation, in the local RBF method they are computed by tting an RBF interpolant through a stencil of neighboring nodes. Both, FD and local RBF formulas are identical in form, and therefore we will refer to the local RBF method as the RBF nite di erence (RBF-FD) method, as was named in [28]. In the last years the RBF-FD method has been successfully applied to a great variety of problems [3,5,6,8 10,17 20,23,25,27].

Most of the RBFs used in the literature for solving PDEs depend on a shape parameter c, and there is much experimental evidence showing that the accuracy of the solution to a PDE strongly depends on the value of this parameter c. In [2], we reviewed some of the main e orts to compute its optimal value, both in the case of using a constant shape parameter at all nodes of the domain, and in the case of using a node-dependent shape parameter. We also described a new technique to compute e ciently the optimal (constant) value of the shape parameter that minimizes the RBF-FD error. The technique was based on the analytical approximations to the local errors in powers of the shape parameter c and nodal distance h derived in [1]. We analytically showed that there was a range of values of the shape parameter c for which the RBF-FD formulas were signi cantly more accurate than the FD ones, and we computed the optimal (constant) value that minimized the truncation error.

This paper is a follow up to the work started in [2]. We present a new and practical algorithm to exploit RBF-FD formulas using a node dependent variable value of the shape parameter. We show that a simple and inexpensive numerical strategy can give rise to several orders of magnitude increase in accuracy if one allows the shape parameter c to be di erent at each node of the domain, instead of using a constant value as in [2]. We also show that, if there are a signi cant number of nodes for which no optimal value of the shape parameter exists, then the improvement in accuracy deteriorates significantly. In those cases, we use generalized multiquadrics as RBFs and choose the exponent of the multiquadric at each node to assure the existence of an optimal variable shape parameter. In this way, we are able to obtain signi - cant accuracy improvements with respect to the optimal constant method for all the example problems analyzed in this work.

The paper is organized as follows. In Section 2, we describe the local RBF method, and we explain how to compute the optimal variable shape parameters. In Section 3, we give the numerical algorithm to compute them. In Section 4, we show examples in one and two dimensions using both structured and unstructured grids. For comparison purposes we use the same examples used in [2]. Finally, Section 7 contains our conclusions.

2 RBF-FD method formulation

Consider the Dirichlet problem in a bounded domain $\mathbb{R}^d$

$$\begin{aligned} \mathcal{L}[u(\mathbf{x})] &= f(\mathbf{x}) \qquad \text{in} \\ u(\mathbf{x}) &= g(\mathbf{x}) \qquad \text{on} \end{aligned} \tag{1}$$

where $\mathcal{L}[\,]$ is a di erential operator, and f and g are real functions. In the RBF-FD method we approximate the operator $\mathcal{L}[\,]$ at a node $\mathbf{x} = \mathbf{x}_j$ by a linear combination of the values of the unknown function u at n scattered nodes surrounding $\mathbf{x}_j$, which constitute its stencil. Thus,

$$\mathcal{L}[u(\mathbf{x}_j)] \quad \sum_{i=1}^{n} \quad _{ji} u(\mathbf{x}_i) \tag{2}$$

where $_{ji}$ are the weighting coe cients. In the standard FD formulation, these coe cients are computed using polynomial interpolation. In the RBF-FD formulation, they are computed using interpolation with radial basis functions, thus

$$u(\mathbf{x}) = \sum_{i=1}^{n} \quad _i \quad (r_i(\mathbf{x}) \;\; c) \tag{3}$$

where $r_i(\mathbf{x}) = \quad \mathbf{x} \quad \mathbf{x}_i \quad$ is the distance from the RBF center, and $\quad (r_i(\mathbf{x}) \;\; c)$ is some radial function which depends on a free shape parameter c. In this paper, we will use Hardy s multiquadric as RBFs [12], so

$$(r_i(\mathbf{x}) \;\; c) \;=\; \quad \overline{c^2 \;+\; r_i(\mathbf{x})^2} \tag{4}$$

Substituting (3) into (2) we can determine the unknown weighting coe cients $_{ji}$ by solving the system of linear equations

$$\mathcal{L}[\;\; (r_k(\mathbf{x}_j) \;\; c)] \;=\; \sum_{i=1}^{n} \quad _{ji} \;\; (r_k(\mathbf{x}_i) \;\; c) \qquad k = 1 \qquad n \tag{5}$$

From these equations, we observe that the coe cients $_{ji}$ depend on the distances from $\mathbf{x}_j$ to the other nodes $\mathbf{x}_i$ in the stencil, and on the shape parameter

c. As we emphasized before, accuracy is highly dependent on the value of this parameter c. Therefore, we allow c to be di erent at each stencil centered at $\mathbf{x}_j$. Thus, we solve

$$\mathcal{L}[\ (r_k(\mathbf{x}_j)\ \ c_j)] = \sum_{i=1}^{n} \ _{ji}\ (r_k(\mathbf{x}_i)\ \ c_j) \qquad k = 1 \qquad n \tag{6}$$

to determine the weighting coe cients $_{ji}$. In the following, we will assume that the set of interpolation nodes with the corresponding stencils are given. Therefore, the coe cients $_{ji}$ will be functions of the shape parameter c_j only.

Suppose that the domain is discretized using N scattered nodes (N_I interior nodes and N N_I boundary nodes). Using (2), Eq. (1) at an interior node $\mathbf{x}_j$ can be written as

$$\sum_{i=1}^{n} \ _{ji}(c_j)u(\mathbf{x}_i) = f(\mathbf{x}_j) + \ _n(\mathbf{x}_j\,; c_j) \qquad 1 \quad j \quad N_I \tag{7}$$

where $_n(\mathbf{x}_j\,;\, c_j)$ is the local RBF-FD error resulting from approximating the di erential operator $\mathcal{L}[\,]$ with the n node RBF-FD formula (2), and c_j is the shape parameter corresponding to the stencil centered at $\mathbf{x}_j$. In matrix form, these equations can be written as

$$A(\mathbf{c})\mathbf{u} = \mathbf{f} + \boldsymbol{\epsilon}(\mathbf{c}) \tag{8}$$

where $\mathbf{u}$ is the vector of exact solutions at the interior nodes, $\mathbf{c}$ is the vector of shape parameters at the interior nodes, $A(\mathbf{c})$ is a N_I N_I sparse matrix whose entries are the weighting coe cients $_{ji}(c_j)$, and $\boldsymbol{\epsilon}(\mathbf{c})$ is a vector formed by the local RBF-FD approximation errors $_n(\mathbf{x}_j\,;\, c_j)$ at the interior nodes.

The RBF-FD approximation $\mathbf{u}$ to the exact solution $\mathbf{u}$ is obtained by formally solving the discretized linear system

$$\mathbf{u}(\mathbf{c}) = A\ ^{1}(\mathbf{c})\,\mathbf{f} \tag{9}$$

so the RBF-FD error is given by

$$\mathbf{E}(\mathbf{c}) \qquad \mathbf{u} \qquad \mathbf{u}(\mathbf{c}) \tag{10}$$

Therefore, we can state our problem as the problem of nding the vector of shape parameters $\mathbf{c}$ which minimizes (10) in a certain norm. We de ne the optimal shape parameter vector as the value $\mathbf{c}$ such that

$$\mathbf{E}(\mathbf{c}\ ) \quad = \min_{\mathbf{c}} \ \mathbf{E}(\mathbf{c}) \qquad \min_{\mathbf{c}} \ \mathbf{u} \qquad \mathbf{u}(\mathbf{c}) \tag{11}$$

It is apparent that in real problems the value $\mathbf{c}$ can not be computed directly from (11) because the exact solution $\mathbf{u}$ is not known. However, from (8) and

(9) we can write

$$\mathbf{E}(\mathbf{c}\ ) \quad = \min_{\mathbf{c}} \quad A\ ^{1}(\mathbf{c})\,\boldsymbol{\epsilon}(\mathbf{c}) \tag{12}$$

and estimate the value $\mathbf{c}$ using the analytical approximations to the local error $\boldsymbol{\epsilon}(\mathbf{c})$ derived in [1]. These formulas are written as series expansions in powers of h (the average inter-nodal distance), which are valid for $c_j \quad h$. The coe cients of these formulas depend on the shape parameter c_j, the distances to the other nodes in the stencil, and on the value of the exact solution and its derivatives at each node $\mathbf{x}_j$. Moreover, these coe cients can be easily computed without losing accuracy using an approximate nite di erence solution $\mathbf{u}$ instead of the exact solution $\mathbf{u}$. Using these formulas, we seek for an approximate value $\mathbf{c}_e$ to the optimal shape parameter vector $\mathbf{c}$ such that

$$\mathbf{E}_e(\mathbf{c}_e) \quad = \min_{\mathbf{c}} \quad A\ ^{1}(\mathbf{c})\,\boldsymbol{\epsilon}_e(\mathbf{c}) \tag{13}$$

where $\boldsymbol{\epsilon}_e(\mathbf{c})$ is the estimated local error computed with the analytical approximations to the local error derived in [1].

Problem (13) is the same type of minimization problem that was solved in [2], but now one has to nd N_i unknown shape parameters at the interior nodes, instead of only one constant shape parameter c as was done in [2]. Furthermore, $A\ ^{1}(\mathbf{c})\,\boldsymbol{\epsilon}_e(\mathbf{c})$ is a scalar function of N_i dimensions with an extremely high number of local minima, so minimization algorithms, such as the routine `fminsearch` of Matlab, are of little use because they immediately fall in one of these local minima.

To compute the global minimum it is necessary to use nonlinear optimization algorithms such as *simulated annealing* [15]. We have used this technique to solve the one dimensional boundary value problem considered as a rst example in [2] (see Eq. (13) in [2]) and we have obtained an error of $\mathbf{E}(\mathbf{c}) \quad = 2\,947\,10\ ^{4}$. This result is signi cantly more accurate than the one obtained with the optimal (constant) shape parameter ($\mathbf{E}(c) \quad = 1\,178\,10\ ^{3}$). However, this procedure is computationally very expensive and, in general, is not capable of nding the absolute minimum of the problem.

Thus, instead of solving problem (13) to nd the vector $\mathbf{c}_e$ that minimizes the estimated error $\mathbf{E}_e(\mathbf{c}) \quad$, we compute the values $\mathbf{c}_e^+$ that minimize the local estimated approximation errors $\boldsymbol{\epsilon}_e(\mathbf{c})$. Since the element j of $\boldsymbol{\epsilon}_e(\mathbf{c})$, $_n(\mathbf{x}_j\,;\,c_j)$, only depends on the shape parameter c_j, minimizing $\boldsymbol{\epsilon}_e(\mathbf{c})$ involves N_I minimization problems with one unknown each, which is a much more tractable problem. In fact, we compute the optimal shape parameter at each interior node $\mathbf{x}_j$ by solving $_n(\mathbf{x}_j\,;\,c_j^+) = 0$. This is a polynomial equation that can be solved analytically using the explicit formulas for the local errors derived in [1].

For an optimal shape parameter c_j^+ to be valid two conditions must be satis ed:

(i) the solution for $_n(\mathbf{x}_j\,;\,c_j^+)=0$ must be real, and (ii) c_j^+ h. If condition (i) is not satis ed there is not a value of the shape parameter for which the local approximation error is zero. If condition (ii) is not satis ed then the optimal value computed is not valid since it is obtained using the local error formulas outside their region of validity. In both cases, we use the standard central nite di erence formula instead.

3 Numerical algorithm

For a given problem (1), and a given set of N scattered nodes, the method described in the previous Section is implemented as follows:

(1) For each interior node $\mathbf{x}_j$ determine a stencil of n surrounding nodes.
(2) Use nite di erences to compute an approximate solution $\mathbf{u}(\mathbf{x}_j)$.
(3) At each interior node $\mathbf{x}_j$, compute the estimated value of the optimal shape parameter, c_j^+, using the approximate formulas derived in [1]. These formulas depend on the value of the function and its derivatives at the node, which are estimated using the nite di erence solution $\mathbf{u}(\mathbf{x}_j)$.
(4) Use (6) to compute the RBF-FD coe cients $_{ji}$ numerically and, therefore, matrix $\mathbf{A}(\mathbf{c}_e^+)$. In nodes where there is not optimal shape parameter use the standard nite di erence coe cients.
(5) Compute the optimal RBF-FD approximate solution $\mathbf{u}(\mathbf{c}_e^+) = A\ ^1(\mathbf{c}_e^+)\,\mathbf{f}$.

4 Example problems in one dimension

In this section, we will apply the numerical algorithm just described to the solution of the same example problems in 1D and 2D that were solved in our previous paper [2] with an optimal (constant) shape parameter. We will use both structured and non structured nodes and we will show that using the optimal node dependent value of the shape parameter leads to further signi cant improvements in accuracy.

4.1 One dimensional boundary value problem

We consider the following problem

$$\begin{aligned} &u_{xx} = f(x) \qquad 0<x<1 \\ &u(0)=1 \qquad u(1)=1+\frac{\overline{2}}{2} \end{aligned} \tag{14}$$

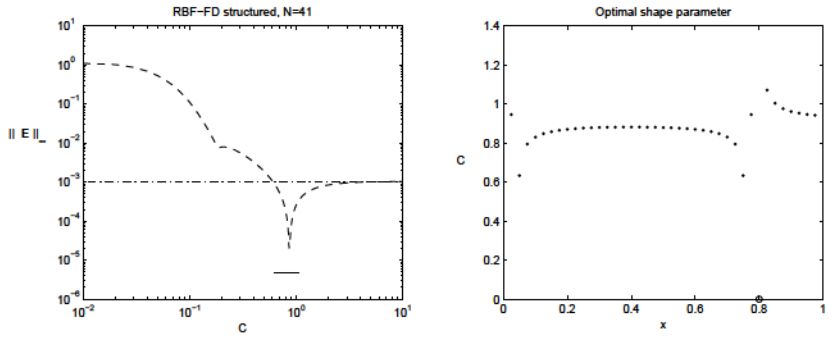

Fig. 1. Left plot: Infinite norm of the errors of problem (14) as function of c, using $N = 41$ structured nodes. Solid line; RBF-FD error with variable c_j^+. Dashed line; RBF-FD error with constant c. Dot-dashed line; FD error. Right plot: $(\cdot)$ optimal shape parameter distribution $\mathbf{c}_e^+$. The nodes where c_j^+ does not exist are marked with a circle $(\circ)$.

where $f(x)$ is computed from the known solution $u(x) = 1 - \sin\left(\frac{5\pi}{4}x\right)$.

4.1.1 Structured nodes

Let us discretize the domain in (14) using $N = 41$ structured nodes, and let us use a three node $(x_j - h, x_j, x_j + h)$ central difference scheme to approximate the second derivative. The resulting local RBF-FD approximation error is [1]

$$\epsilon_3(x_j; c_j) = \frac{h^2}{12}\, u^{(IV)}(x_j) + \frac{h^2}{c_j^2}\, u''(x_j) - \frac{3\,h^2}{4\,c_j^4}\, u(x_j) + O\left(h^4\, P_3(1/c_j^2)\right) \quad (15)$$

We use the notation $O\left(h^m\, P_n(1/c^2)\right)$ to indicate that the terms that have been neglected are of order $h^m \sum_{i=0}^{n} \frac{a_i}{c^{2i}}$, where a_i are constants which depend on the derivatives and values of the particular function at x_j.

To estimate this error we use a second order finite difference approximation $\tilde{u}(x_j)$ to the exact solution $u(x_j)$, so $\tilde{u}(x_j) = u(x_j) + O(h^2)$. In (15), $u''(x_j)$ and $u^{(IV)}(x_j)$ are computed exactly from $f(x_j)$, so

$$\tilde{\epsilon}_3(x_j; c_j) = \frac{h^2}{12}\, f''(x_j) + \frac{h^2}{c_j^2}\, f(x_j) - \frac{3\,h^2}{4\,c_j^4}\, \tilde{u}(x_j)\,. \quad (16)$$

The accuracy of the local error computed with the finite-difference approximation in (16) is of the same order $(O(h^4))$ as the one computed with the exact solution in (15). The optimal shape parameters c_j^+ are computed equating (16) to zero for every node x_j.

Table 1
RBF-FD results for problem (14): N is the number of nodes; $\min(\mathbf{c}_e^+)$ and $\max(\mathbf{c}_e^+)$ are the minimum and maximum values of the optimal shape parameters c_j^+; $\%N$ and $\mathbf{E}(\mathbf{c}_e^+)$ are the percentage of nodes for which c_j^+ does not exist and the corresponding in nite norm of the error; c_e and $\mathbf{E}(c_e)$ are the optimal constant shape parameter and the corresponding in nite norm of the error; $\mathbf{E}$ is the in nite norm of the conventional nite di erences.

Structured nodes									
N	$\min(\mathbf{c}_e^+)$	$\max(\mathbf{c}_e^+)$	$\%N$	$\mathbf{E}(\mathbf{c}_e^+)$		c_e	$\mathbf{E}(c_e)$		$\mathbf{E}$
21	0.6326	1.0039	4.8	3 698	10^{-5}	0.8628	7 763	10^{-5}	4 181 10^{-3}
41	0.6333	1.0712	2.4	4 728	10^{-6}	0.8626	1 735	10^{-5}	1 044 10^{-3}
61	0.6334	1.1789	1.6	1 959	10^{-6}	0.8625	7 541	10^{-6}	4 638 10^{-4}
81	0.6334	1.3730	1.2	1 083	10^{-6}	0.8625	4 216	10^{-6}	2 609 10^{-4}
Unstructured nodes									
N	$\min(\mathbf{c}_e^+)$	$\max(\mathbf{c}_e^+)$	$\%N$	$\mathbf{E}(\mathbf{c}_e^+)$		c_e	$\mathbf{E}(c_e)$		$\mathbf{E}$
21	0.2760	1.0596	0	2 211	10^{-4}	0.7858	1 207	10^{-3}	4 928 10^{-3}
41	0.3962	1.3382	0	2 625	10^{-6}	0.7959	1 981	10^{-4}	1 327 10^{-3}
61	0.3965	1.4689	0	2 516	10^{-6}	1.0069	4 586	10^{-5}	3 818 10^{-4}
81	0.3715	1.7317	1.2	3 348	10^{-6}	0.8071	2 595	10^{-5}	3 377 10^{-4}

In the left plot of Fig. 1 we show with a dashed line the in nity norm of the RBF-FD error, $\mathbf{E}(c) = \mathbf{u} \quad \mathbf{u}(c)$, using a constant shape parameter c throughout the domain. Notice that in the limit of increasingly at basis functions (c) the RBF-FD error approaches the standard nite di erence one [29], shown with a dot-dashed line in the gure. The in nity norm of the RBF-FD error using the algorithm described in Section 3 is shown with a solid line. The length of the line represents the range of the optimal values of the shape parameters c_j^+. Notice that the accuracy is slightly higher with the variable shape parameter than with the constant one.

The right plot of Fig. 1 shows the distribution of the optimal shape parameters. These values are quite close to the value of the optimal (constant) shape parameter $c = 0\,8626$. Only near $x = 0$ and $x = 0\,8$ the local optimal values c_j^+ di er signi cantly from the constant value. This explains why, in this case, there is not a very signi cant improvement in accuracy using a variable shape parameter. Also notice that for $x_j = 0\,8$ there is not a real value c_j^+ that satis es $_3(x_j; c_j^+) = 0$. These nodes are marked with the symbol in the gure.

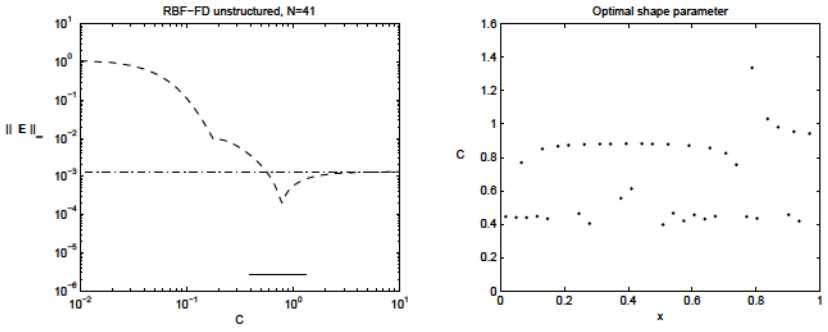

Fig. 2. Same as Fig. 1 but for unstructured nodes.

Table 1 shows results for different values of N. The second and third columns display the minimum and maximum values of the optimal shape parameters c_j^+, respectively, the forth column the percentage of nodes for which c_j^+ does not exist ($\%\, N$), and the fifth column the infinite norm of the error $||\mathbf{E}(\mathbf{c}_e^+)||_\infty$. For comparison, we show in the sixth and seventh columns the corresponding results for the optimal (constant) shape parameter (c_e^* and $||\mathbf{E}(c_e^*)||_\infty$, respectively), and in the last column the results for conventional finite differences ($||\tilde{\mathbf{E}}||_\infty$). For all values of N, there is some improvement in accuracy using the variable optimal shape parameter instead of the constant optimal one.

4.1.2 Unstructured nodes

When the domain is discretized with unequally spaced nodes, the local RBF-FD approximation error using a three node $(x_j - h, x_j, x_j + \lambda h)$ central difference scheme is only of order $O(h)$ (see [1]), so we also include terms of order $O(h^2)$ in the formula. Therefore, the truncation error is of order $O(h^3)$, while in the case of structured nodes it was of order $O(h^4)$. The estimated local error is

$$\begin{aligned}\tilde{\epsilon}_3(x_j; c_j) = &\frac{\lambda - 1}{3} h\, f'(x_j) + (\lambda - 1)\, \frac{h}{c_j^2}\, \tilde{u}'(x_j) \\ &+ [\lambda\,(\lambda - 1) + 1]\, \frac{h^2}{12}\, f''(x_j) + \lambda \frac{h^2}{c_j^2}\, f(x_j) \\ &+ [\lambda\,(\lambda - 5) + 1]\, \frac{h^2}{4\, c_j^4}\, \tilde{u}(x_j)\,, \end{aligned} \tag{17}$$

where we have used (14) to replace $u^{(k)}$, $k \geq 2$, by the function f and its derivatives. We have also replaced the exact solution u and its first derivative u' by the first order finite difference approximations $\tilde{u}$ and $\tilde{u}'$, respectively. In this case, $\tilde{u}'$ is computed from $\tilde{u}$ using a first order finite difference approximation. This procedure does not introduce higher order errors.

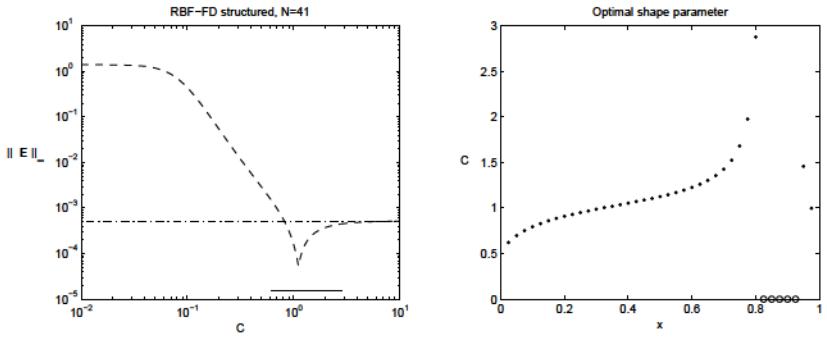

Fig. 3. Same as Fig. 1 but for problem (18).

In Fig. 2, we show the results from problem (14) using $N = 41$ unstructured nodes. The left plot shows the infinity norms of the RBF-FD error using a constant shape parameter (dashed line), and using the algorithm described in Section 3 (solid line). The length of the solid line represents the range of the optimal variable values c_j^+. In this case, there is an improvement of approximately two orders of magnitude between the results for a constant shape parameter and the results for a variable one. The right plot of the figure shows the distribution of optimal shape parameters, which range from 0.4 to 1.4. The optimal constant shape parameter is, in this case, $c^* = 0.7959$ [1], which is a kind of average of the optimal variable values shown in the figure.

The results for different values of N are summarized in the bottom part of Table 1. For all the resolutions reported here, there is an order of magnitude of improvement with respect to the results obtained with a constant optimal shape parameter. This improvement is due to the fact that an optimal value c_j^+ exists for all nodes (except for $N = 81$).

4.2 Steady convection-diffusion problem

Consider the problem

$$\begin{cases} u_x - u_{xx} = \pi^2 \sin(\pi x) + \pi \cos(\pi x), & 0 < x < 1, \\ u(0) = 0, \qquad u(1) = 1 \end{cases} \tag{18}$$

whose exact solution is $u(x) = \sin(\pi x) + \dfrac{e^x - 1}{e - 1}$. This problem was proposed and solved in [4].

Table 2
Same as Table 1 but for the steady convection-di usion problem (18).

Structured nodes							
N	$\min(\mathbf{c}_e^+)$	$\max(\mathbf{c}_e^+)$	$\%\,N$	$\mathbf{E}(\mathbf{c}_e^+)$	c_e	$\mathbf{E}(c_e)$	$\mathbf{E}$
11	0.7963	2.8808	9.0	1 719 10 ^{4}	1.1139	9 245 10 ^{4}	8 337 10 ^{3}
21	0.6979	2.8796	9.5	5 643 10 ^{5}	1.1127	2 161 10 ^{4}	2 088 10 ^{3}
41	0.6224	2.8793	12.2	1 523 10 ^{5}	1.1123	5 282 10 ^{5}	5 220 10 ^{4}
81	0.5707	5.8510	11.1	3 834 10 ^{6}	1.1123	1 314 10 ^{5}	1 305 10 ^{4}
Unstructured nodes							
N	$\min(\mathbf{c}_e^+)$	$\max(\mathbf{c}_e^+)$	$\%\,N$	$\mathbf{E}(\mathbf{c}_e^+)$	c_e	$\mathbf{E}(c_e)$	$\mathbf{E}$
11	0.9933	3.3864	54.5	1 008 10 ^{2}	1.1409	5 060 10 ^{3}	1 105 10 ^{2}
21	0.8469	3.2638	57.1	1 525 10 ^{3}	0.9818	4 832 10 ^{4}	2 667 10 ^{3}
41	0.6074	2.2497	31.7	2 843 10 ^{4}	1.0536	5 979 10 ^{5}	6 788 10 ^{4}
81	0.4002	3.9330	25.9	1 026 10 ^{4}	1.0539	1 584 10 ^{5}	1 685 10 ^{4}

4.2.1 Structured nodes

The local estimated approximation error to the convection-di usion di erential operator with the RBF-FD formula using three structured nodes is

$$
\begin{aligned}
{}_3(x_j; c_j) = \frac{h^2}{12} \quad & 2\,u \ \ (x_j) \quad\quad u^{(IV)}(x_j) \quad + \frac{h^2}{2c_j^2}\,(u\,(x_j) \quad\quad 2\,u\ \ (x_j)\,) \\
& + \frac{3\,h^2}{4\,c_j^4}\,u(x_j)
\end{aligned}
\tag{19}
$$

In this formula, u is a second order nite di erence approximation of u and u is approximated from u using the corresponding second order central difference scheme. Higher derivatives are approximated to second order through the recursion $u^{(k+1)} = u^{(k)} \quad f^{(k\ \ 1)}$ for $k \quad 1$.

In Fig. 3, we show the results from problem (18) using 41 nodes of the discretization. The left plot shows the in nity norm of the RBF-FD error using a constant shape parameter (dashed line) and the in nity norm of the RBF-FD error using the algorithm described in Section 3 (solid line). The length of this line represents the range of the optimal values of the shape parameters c_j^+ (between 0 6 and 3, approximately). The results for $N = 41$ and for other values of N are summarized in Table 2. Notice that there is only a small improvement with respect to the results obtained with the optimal constant

Table 3
Same as Table 1 but for the steady convection-di usion problem (20).

Structured nodes							
N	$\min(\mathbf{c}_e^+)$	$\max(\mathbf{c}_e^+)$	$\%\, N$	$\mathbf{E}(\mathbf{c}_e^+)$	c_e	$\mathbf{E}(c_e)$	$\mathbf{E}$
11	2.2171	2.4195	0	3 466 10 ^{7}	2.3065	1 463 10 ^{6}	1 007 10 ^{4}
21	2.2060	2.4343	0	2 175 10 ^{8}	2.3066	3 266 10 ^{7}	2 515 10 ^{5}
41	2.2006	2.4419	0	1 793 10 ^{9}	2.3065	7 786 10 ^{8}	6 292 10 ^{6}
61	2.1988	2.4444	0	1 230 10 ^{9}	2.3065	3 418 10 ^{8}	2 797 10 ^{6}
Unstructured nodes							
N	$\min(\mathbf{c}_e^+)$	$\max(\mathbf{c}_e^+)$	$\%\, N$	$\mathbf{E}(\mathbf{c}_e^+)$	c_e	$\mathbf{E}(c_e)$	$\mathbf{E}$
11	2.2125	2.3608	54.5	3 812 10 ^{4}	9 3362 10^{1}	3 8526 10 ^{4}	3 907 10 ^{4}
21	2.2101	2.4084	52.3	3 397 10 ^{5}	3.3788	4 093 10 ^{5}	4 722 10 ^{5}
41	2.2023	2.4297	46.3	5 099 10 ^{6}	2.4715	5 216 10 ^{6}	9 431 10 ^{6}
61	2.1988	2.4445	3.3	3 325 10 ^{6}	1.7107	4 107 10 ^{6}	5 723 10 ^{6}

value of the shape parameter (c = 1 1123). The reason for these results can be explained by looking at the optimal shape parameter distribution shown in the right plot of this gure. Observe that there are ve nodes, in the vicinity of x = 0 85, for which no optimal shape parameter exists. In these nodes, standard nite di erence formulas are used to approximate the convection-di usion di erential operator. This approximation deteriorates signi cantly the overall accuracy. Similar results are obtained for other values of N, as can be seen in Table 2. In fact, we have observed that the accuracy obtained with the algorithm described in Section 3 is highly dependent on the number of nodes for which c_j^+ exists. If there are very few nodes for which c_j^+ does not exist, then the improvement of the accuracy compared to standard FD is very high. However, if there are many nodes for which c_j^+ does not exist then the accuracy is similar to that obtained with an optimal constant c or even with standard FD formulas.

Let us corroborate this behavior by considering the following steady convection-di usion problem

$$\begin{aligned} & u_x \quad u_{xx} = 0 \qquad 0 < x < 1 \\ & u(0) = 0 \qquad u(1) = 1 \end{aligned} \tag{20}$$

whose exact solution is $u(x) = \dfrac{e^x \quad 1}{e \quad 1}$. This problem was also proposed and solved in [4].

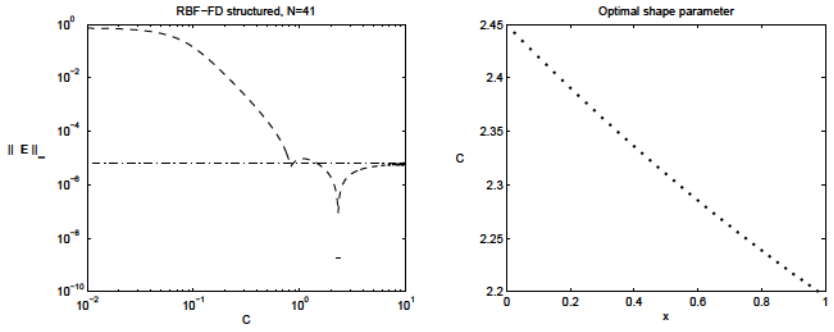

Fig. 4. Same as Fig. 1 but for problem (20).

The left plot of Fig. 4 shows the corresponding errors for this problem. Notice that, in this case, there is a very significant improvement of two orders of magnitude in accuracy. The reason for this improvement can be understood by considering the optimal shape parameter distribution which is shown in the right plot of Fig. 4. For all the nodes there is a value c_j^+ of the shape parameter for which the local approximation error (19) has a minimum. It is remarkable that although the values of c_j^+ are relatively constant ($2.20 \leq c_j^+ \leq 2.44$, for all j), those small variations suffice to produce a considerable increase in accuracy. Similar accuracy improvements are obtained for other values of N (see Table 3) since in all cases there exits an optimal value c_j^+ in each node ($\% N = 0$).

4.2.2 Unstructured nodes

In the case that the domain is discretized with unequally spaced nodes, the local estimated RBF-FD approximation error using a three node $(x - h, x, x + \lambda h)$ central difference scheme for the convection-diffusion operator is

$$\begin{aligned}\tilde{\epsilon}_3(x_j; c_j) = & \frac{(1-\lambda)}{3} h\, \tilde{u}'''(x_j) + (1-\lambda)\, \frac{h}{c_j^2}\, \tilde{u}'(x_j) \\ & + \frac{h^2}{12} \left[2\,\lambda\, \tilde{u}'''(x_j) - [\lambda\,(\lambda-1)+1]\, \tilde{u}^{(IV)}(x_j) \right] \\ & + \frac{\lambda\, h^2}{2\, c_j^2} \left[\tilde{u}'(x_j) - 2\, \tilde{u}''(x_j) \right] - [\lambda\,(\lambda-5)+1]\, \frac{h^2}{4\, c_j^4}\, \tilde{u}(x_j). \quad (21)\end{aligned}$$

Function $\tilde{u}$ and its derivatives are approximated as described in the previous section.

In Fig. 5, we show the results from problem (18) using 41 unstructured Halton nodes. The left plot shows the infinity norm of the RBF-FD error using a constant shape parameter (dashed line) and the infinity norm of the RBF-FD error using the algorithm described in Section 3 (solid line). The length of

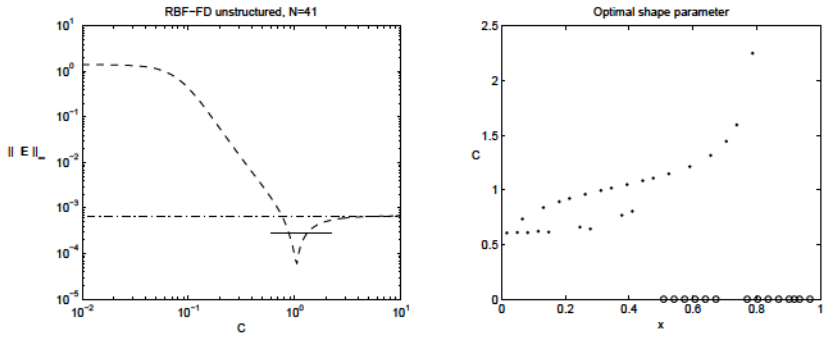

Fig. 5. Same as Fig. 3 but for 41 unstructured Halton nodes.

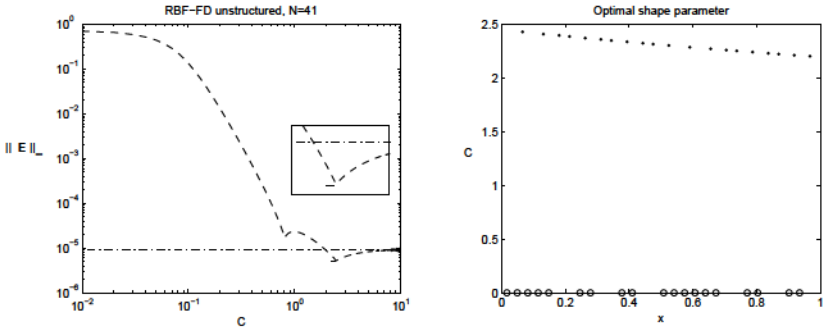

Fig. 6. Same as Fig. 4 but for 41 unstructured Halton nodes.

the line shows the range of the optimal values of the shape parameters c_j^+ (between approximately 0.6 and 2.3). The right plot shows the optimal shape parameter distribution. Notice that there is a significant number of nodes for which an optimal value of the shape parameter c_j^+ does not exist (31.7 %) and, therefore, the standard finite difference approximation is used at those nodes. As a result, the overall accuracy of the solution is degraded in comparison with the optimal constant shape parameter. Similar results are obtained for other values of N, as can be seen in the bottom part of Table 2.

Figure 6 shows the corresponding results for problem (20). Observe in the right plot of this figure that for approximately half of the nodes (46.3 %) an optimal value c_j^+ exists ($2.2 \leq c_j^* \leq 2.45$), while for the other half no c_j^+ exists. The resulting overall accuracy is very similar to that obtained with the optimal constant shape parameter technique [2]. Similar results are obtained for other values of N as can be seen in the bottom part of Table 3.

It should be mentioned that in some of the nodes marked with the symbol '$\circ$', there are values of the shape parameter for which the local approximation errors (21) are minimum. However, the resulting shape parameters are small, and do not satisfy the assumption $c \gg h$ for which the formulas derived in [1] are valid. Thus, for those values of c, Eq. (21) is not a good approximation to the local approximation error and, therefore, it can not be used to compute a valid c_j^+. Accordingly, we only accept the c_j^+ values that satisfy the condition

$c_j^+ > c_{min}$ h, where c_{min} is a previously de ned threshold. Hence, item 4 of the numerical algorithm in Section 3 is substituted by

4. Use (6) to compute numerically the RBF-FD coe cients $_{ji}$ and therefore matrix $\mathbf{A}(\mathbf{c}_e^+)$. In nodes where there is not an optimal shape parameter or where $c_j^+ < c_{min}$, use standard nite di erence coe cients.

In Figure 6 and Table 3 we have used $c_{min} = 0\ 5$. We will use this modi ed algorithm in the rest of the paper.

5 Generalized multiquadrics.

From the previous results, it is apparent that the use of a variable shape parameter can give rise to several orders more accurate solutions if a valid c_j^+ exists at almost all nodes of the computational domain. However, very often, there are nodes for which no c_j^+ h exists for which the leading order of the local RBF-FD multiquadric based approximation (Eqs. (19) and (21) in this Section) is zero. Hence, we propose the use of another RBF that ensures that the RBF-FD local approximation error is zero to leading order at all nodes. To this end, one possibility that we have successfully used is the generalized multiquadric

$$(r_i(\mathbf{x})\ c\quad) = (c^2 + r_i(\mathbf{x})^2)\quad ^2 \tag{22}$$

where the new (node-dependent) parameter is chosen so that an optimal value c_j^+ h exists at every node. For the steady convection-di usion problem (18), the local RBF-FD error formula analogous to (21) is

$$\begin{aligned}
{}_3(x_j; c_j\quad {}_j) = {} & \frac{(1\qquad)}{3}\, h\, u\ \ (x_j) + \frac{h}{c_j^2}(\ {}_j\quad 2)(\qquad 1)\, u\,(x_j) \\
& + \frac{h^2}{12}\quad 2\quad u\ \ (x_j)\qquad [\quad (\qquad 1) + 1]\ u^{(IV)}(x_j) \\
& + \frac{h^2}{c_j^2}\ \frac{(2\qquad {}_j)}{2}\ \ u\,(x_j) + \frac{(\ {}_j\quad 2)}{6(\ {}_j\quad 3)}\quad {}_j\quad ^2 + \quad + 1\qquad (\quad + 13)\quad 1\ \ u\ \ (x_j) \\
& + \frac{h^2}{c_j^4}\,\frac{(\ {}_j\quad 7)(\ {}_j\quad 2)}{12\,(\ {}_j\quad 3)}\ {}_j\,[\ (\qquad 5) + 1]\ u(x_j) + O\ \ h^3\, P_2(1\ \ c_j^2)
\end{aligned} \tag{23}$$

The error is now a function of h c_j and $_j$. The objective is to nd at each node x_j a valid combination of values $(c_j^+\quad {}_j^+)$ for which the leading order of the local RBF-FD error is zero. For a given $_j$ equating to zero the leading order equation for the local error (23) results in a polynomial equation of second degree in the variable $1\ \ c_j^2$ that we solve analytically. This

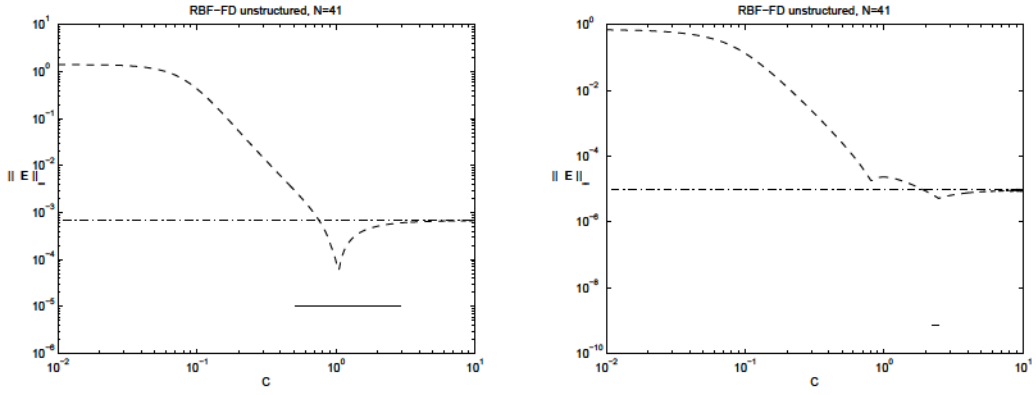

Fig. 7. Results for the convection-diffusion problems using the generalized multiquadric (22). Left: same as Fig. 5 (problem (18)). Right: same as Fig. 6 (problem (20)).

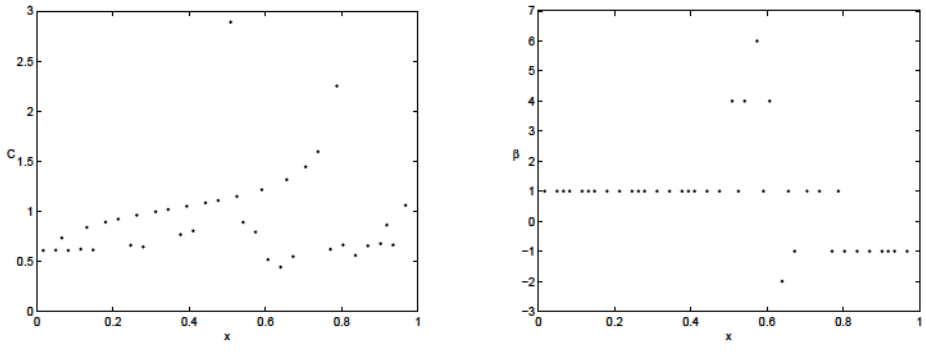

Fig. 8. Optimal shape parameter distribution c_β^+ (left) and β^+ parameter distribution (right) for the convection-diffusion problem (18) using the generalized multiquadric (22).

guarantees, in general, two branches of solutions $c_j^+ = c_j^+(\beta_j^+)$. Hence, there are an infinite number of possible combinations (c_j^+, β_j^+) that make the leading order of the local RBF-FD error zero. However, only those for which c_j^+ is real and $c_j^+ \gg h$ are valid. Between all these possible combinations, we only accept the minimum integer value $\left|\beta_j^+\right|$ which satisfies c_j^+ real and $c_j^+ > c_{min}$. Other strategies, as for instance allowing β_j^+ to be a continuous real variable, are also possible and give the same degree of accuracy.

The left plot of Fig. 7 shows the error of the solution of problem (18) with 41 unstructured Halton nodes, using (22) instead of (4) and $c_{min} = 0.5$. The left plot of Fig. 8 shows the corresponding optimal shape parameter distribution $\left(c_\beta^+\right)_j$ and the right side of Fig. 8 the optimal β_j^+ distribution. These results should be compared to those obtained with the standard multiquadric RBF which are shown in the left plot of Fig. 5. Using the generalized multiquadric (22), a valid value of $\left(c_\beta^+\right)_j$ exists for all nodes and this leads to a significant

Table 4
RBF-FD results for the steady convection-di usion problem (18) with the generalized multiquadric: N is the number of nodes; $\%\,N$ and $\mathbf{E}(\mathbf{c}^+)$ are the percentage of nodes for which $(c^+)_j$ does not exist and the corresponding in nite norm of the error; $\%\,N$ and $\mathbf{E}(c_e^+)$ are the percentage of nodes for which c_j^+ does not exist and the corresponding in nite norm of the error; $\mathbf{E}(c_e)$ is the in nite norm of the error using an optimal constant shape parameter c_e.

Unstructured nodes (beta variable)					
N	$\%\,N$	$\mathbf{E}(\mathbf{c}^+)$	$\%\,N$	$\mathbf{E}(\mathbf{c}_e^+)$	$\mathbf{E}(c_e)$
11	0	8 860 10 ^{4}	54.5	1 008 10 ^{2}	5 060 10 ^{3}
21	0	1 443 10 ^{4}	57.1	1 525 10 ^{3}	4 832 10 ^{4}
41	0	1 001 10 ^{5}	31.7	2 843 10 ^{4}	5 979 10 ^{5}
81	0	4 623 10 ^{7}	25.9	1 026 10 ^{4}	1 584 10 ^{5}

increase in accuracy with respect to the optimal constant shape parameter result. In fact, using (22) the resulting error is $\mathbf{E}(\mathbf{c}^+) = 1\,001\ 10^{-5}$, while using the standard multiquadric (4) the error is $\mathbf{E}(\mathbf{c}_e^+) = 2\,843\ 10^{-4}$. Table 4 shows the corresponding results for other values of N.

The right plot of Fig. 7 shows the error in the solution of problem (20) with 41 unstructured Halton nodes, using (22) instead of (4) and $c_{min} = 0\,5$ Again, a valid value of c_j^+ exists for all nodes and this leads to an even larger improvement in accuracy with respect to the results obtained with standard multiquadrics: $\mathbf{E}(\mathbf{c}^+) = 6\,930\ 10^{-10}$ instead of $\mathbf{E}(\mathbf{c}_e^+) = 5\,099\ 10^{-6}$. This represents four orders of magnitude increase in accuracy.

6 Example problems in two dimensions

Consider now the two dimensional Poisson problem

$$\begin{aligned} u &= f(x\ y) && \text{in} \quad = (0\ 1) \quad (0\ 1) \\ u &= u(x\ y) && \text{on} \end{aligned} \tag{24}$$

where $f(x\ y)$ is obtained from the exact solution

$$u = \exp \quad x \quad \frac{1}{4}^{\ 2} \quad y \quad \frac{1}{2}^{\ 2} \cos(2 \quad y) \sin(\quad x) \tag{25}$$

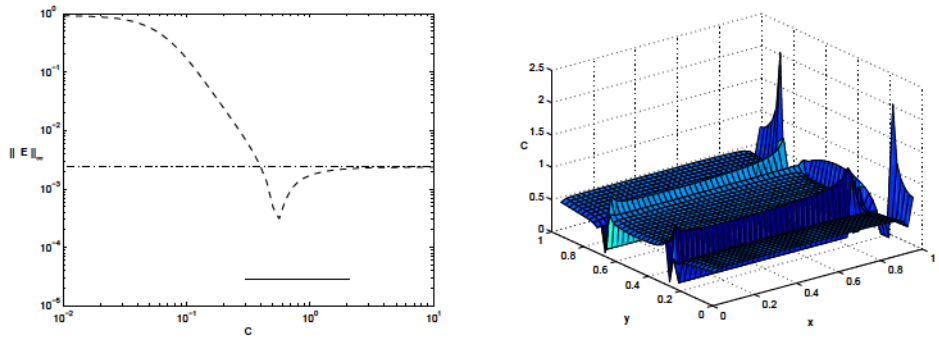

Fig. 9. Left: infinite norm of the errors of problem (24) with exact solution (25) as function of c, using $N = 41 \times 41$ structured nodes. Solid line; RBF-FD error with optimal variable $\mathbf{c}$. Dashed line; RBF-FD error with constant c. Dot-dashed line; FD error. Right: optimal shape parameter distribution $\mathbf{c}_e^+$.

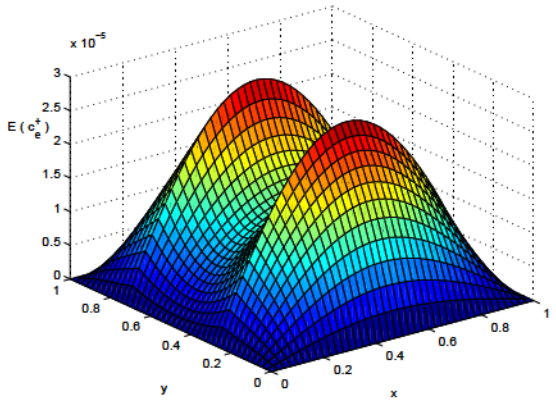

Fig. 10. Absolute RBF-FD global error of problem (24) computed with the optimal shape parameter distribution $\mathbf{c}_e^+$.

This problem has been used by Wright and Fornberg [29] to test the performance of the local RBF-FD and local RBF-HFD (Hermite RBF) methods. We have also used it as an example problem to test the performance of the RBF-FD method using an optimal constant shape parameter [2].

6.1 Structured nodes

Suppose the domain is discretized using an $N \times N$ structured nodes. Using a five node $\{(x, y), (x - h, y), (x + h, y), (x, y - h), (x, y + h)\}$ scheme, the local estimated RBF-FD error is

$$\tilde{\epsilon}_5(\mathbf{x}_j, c_j) = \frac{h^2}{12}\left(\tilde{u}^{(4,0)}(\mathbf{x}_j) + \tilde{u}^{(0,4)}(\mathbf{x}_j)\right) + \frac{5\,h^2}{6\,c_j^2}\,f(\mathbf{x}_j) - \frac{7\,h^2}{6\,c_j^4}\,\tilde{u}(\mathbf{x}_j). \quad (26)$$

Table 5
Same as Table 1 but for the laplacian problem (24)-(25).

Structured nodes											
N		$\min(\mathbf{c}_e^+)$	$\max(\mathbf{c}_e^+)$	$\%\, N$	$\mathbf{E}(\mathbf{c}_e^+)$		c_e	$\mathbf{E}(c_e)$		**E**	
11	11	0.4127	0.7979	1.7	2 422	10^{-3}	0.5779	6 581	10^{-3}	3 847	10^{-2}
21	21	0.3317	0.8835	0.5	1 498	10^{-4}	0.5816	1 352	10^{-3}	9 516	10^{-3}
31	31	0.2146	6.1387	0.2	1 171	10^{-4}	0.5816	5 641	10^{-4}	4 220	10^{-3}
41	41	0.1680	2.0905	4.3	2 810	10^{-5}	0.5818	3 121	10^{-4}	2 370	10^{-3}
Unstructured nodes											
N		$\min(\mathbf{c}_e^+)$	$\max(\mathbf{c}_e^+)$	$\%\, N$	$\mathbf{E}(\mathbf{c}_e^+)$		c_e	$\mathbf{E}(c_e)$		**E**	
121	(120)	0.1220	3.1054	41.3	1 415	10^{-2}	0.4869	1 519	10^{-2}	6 153	10^{-2}
441	(438)	0.1141	3.2097	30.6	7 616	10^{-3}	0.7783	1 079	10^{-2}	1 668	10^{-2}
961	(955)	0.1041	9.0912	26.5	5 796	10^{-3}	0.5058	1 911	10^{-3}	7 454	10^{-3}
1521	(1513)	0.1001	2.9971	29.3	5 239	10^{-3}	0.5094	1 630	10^{-3}	3 983	10^{-3}

In this equation u is a second order approximation of u and $u^{(4\,0)} + u^{(0\,4)} = f \quad 2u^{(2\,2)}$, where $u^{(2\,2)}$ is approximated from u using the corresponding second order central di erence scheme.

In Fig. 9, we show the results from problem (24)-(25) using 41 41 structured nodes and the standard multiquadrics (4). The left plot shows, with a dashed line, the in nity norm of the RBF-FD error using a constant shape parameter throughout the domain. The in nity norm of the RBF-FD error using the algorithm described in Section 3 is shown with a solid line. The length of this line represents the range of the values of the shape parameters c_j^+. Although for most nodes, the values of the c_j^+ are close to the optimal constant shape parameter $c \quad = 0\ 5818$ (see Table 5), the accuracy with the variable shape parameter is signi cantly higher than with the optimal constant one.

The right plot of the gure shows the distribution of the optimal shape parameters c_j^+. In this gure, there are two small intervals in the vicinities of $x = 0\ 25$ and $x = 0\ 75$ for which c_j^+ does not exist. In Fig. 10, we represent the corresponding absolute RBF-FD global error distribution for this example. The maximum error is located at these nodes.

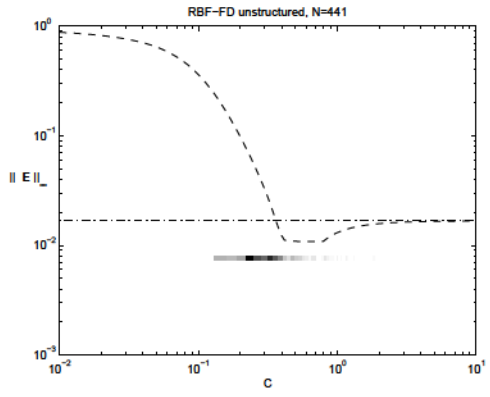

Fig. 11. Same as Fig. 9 but for $N = 441$ unstructured nodes.

6.2 Unstructured nodes

Consider now the case in which the domain is discretized using N unstructured nodes. The local RBF-FD error for six unequally spaced nodes $\{(x,y),(x+h,y+\lambda_1 h),(x+\gamma_2 h,y+\lambda_2 h),(x+\gamma_3 h,y+\lambda_3 h),(x+\gamma_4 h,y+\lambda_4 h),(x+\gamma_5 h,y+\lambda_5 h)\}$ central difference scheme is given by (see reference [1])

$$\begin{aligned}
\epsilon_6(\mathbf{x}_j,c_j) = h\,\Big[A_{0,0}\,u^{(3,0)}(\mathbf{x}_j) \;+\; A_{0,1}\,u^{(2,1)}(\mathbf{x}_j) \\
+ A_{0,2}\,u^{(1,2)}(\mathbf{x}_j) \;+\; A_{0,3}\,u^{(0,3)}(\mathbf{x}_j)\Big] \\
+\frac{h}{c_j^2}\,\Big[A_{1,0},u^{(1,0)}(\mathbf{x}_j) \;+\; A_{1,1}\,u^{(0,1)}(\mathbf{x}_j)\Big] \\
+\,h^2\,\Big[B_{0,0}\,u^{(4,0)}(\mathbf{x}_j) \;+\; B_{0,1}\,u^{(3,1)}(\mathbf{x}_j) \;+\; B_{0,2}\,u^{(2,2)}(\mathbf{x}_j) \\
+ B_{0,3}\,u^{(1,3)}(\mathbf{x}_j) \;+\; B_{0,4}\,u^{(0,4)}(\mathbf{x}_j)\Big] \\
+\frac{h^2}{c_j^2}\,\Big[B_{1,0},u^{(2,0)}(\mathbf{x}_j) \;+\; B_{1,1}\,u^{(1,1)}(\mathbf{x}_j) \;+\; B_{1,2}\,u^{(0,2)}(\mathbf{x}_j)\Big] \\
+\frac{h^2}{c_j^4}\,B_{2,0}\,u(\mathbf{x}_j) \;+\; O\left(h^3\,P_3(1/c_j^2)\right), \qquad (27)
\end{aligned}$$

where the coefficients $A_{i,j}$ and $B_{i,j}$ depend on the surrounding nodes layout $\{\gamma_k\}$ and $\{\lambda_k\}$, and their exact values can be computed numerically for each node. In this example, we have not estimated the derivatives of $u(\mathbf{x})$ that appear in (27) from the numerical solution computed with standard FD. Instead, we have used the exact values of the function and its derivatives in order to analyze the convergence of the error and to estimate the optimal shape parameter.

We use an unstructured node layout of N^2 nodes: $N^2 \quad 4(N \quad 1)$ Halton nodes in the interior of the domain [11], and $4(N \quad 1)$ structured nodes on the boundary. For the local support, we use stencils with $n = 6$ nodes. For standard nite di erences, 6 nodes stencils allow, in principle, a consistent approximation to the laplacian operator (i.e. the approximation is at least rst order accurate) since there are six constraints that have to be satis ed. However, there are special con gurations of the nodes in the stencil for which there is no solution to the constraints [21] and, therefore, the coe cients of the nite di erence formula can not be computed. The problem of stencil support selection for unstructured nodes is a very crucial topic in nite di erences which has been addressed by several authors. In a recent paper, Davydov and Oanh [6] reviewed di erent support selection methods and proposed a new algorithm based on minimizing the sum of the squares of the angles between two consecutive lines from the central node to the other nodes in the stencil.

In this paper, we use a modi ed version of the algorithm recently proposed by Seibold [22]. It is based on a linear programming approach that guarantees the positivity of the stencil. Applying this algorithm, results in a 6 node stencil selection for almost all the interior nodes. Nevertheless, there are a few nodes, usually very close to the boundary, for which this algorithm does not yield a solution. Those nodes are removed from the set, and the algorithm is applied again until a valid nite di erence 6 node stencil is assigned to each node. In the rst column of Table 5 it is shown the number of nodes in the grid, and in parenthesis the number of nodes remaining after applying the algorithm in [22]. Starting from valid nite di erence stencils insures the validity of the corresponding RBF-FD stencils.

Figure 11 shows the in nite norms of the RBF-FD errors of problem (24)-(25) using a constant shape parameter (dashed line), and using the algorithm described is Section 3 (bar). The gray scale in the bar is proportional to the number of nodes with that optimal shape parameter c_j^+. In this case, we have used 21 21 unstructured Halton nodes. Notice that there is a slight improvement of accuracy with respect to the optimal (constant) RBF-FD solution. For more points the accuracy does not improve (see Table 5).

6.3 Additional Poisson equation examples

In this section, we address the solution of several problems de ned by the Poisson equation which have been proposed in the past. In all problems, we consider Eq. (24) with the function f computed, in each case, from the following exact solutions:

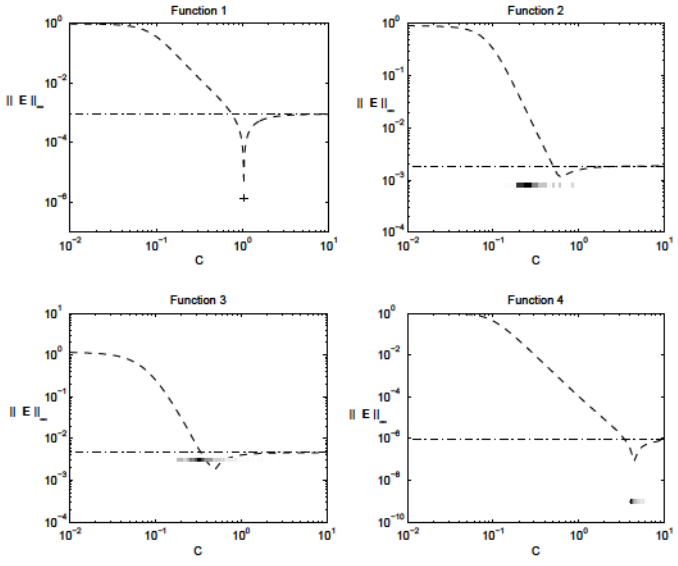

Fig. 12. Infinite norm of the errors of problem (24) with exact solutions (28) to (31), using $N = 31 \times 31$ structured nodes. Dashed line; RBF-FD error with constant c. Dot-dashed line; finite difference error. Bar: RBF-FD error with optimal variable c (the gray scale in the bar is proportional to the number of nodes with a particular shape parameter).

$$u_1 = \sin(\pi x)\sin(\pi y)\,, \tag{28}$$

$$u_2 = \frac{\arctan\left[2(x+3y-1)\right]}{\arctan\left[2(\sqrt{10}+1)\right]}\,, \tag{29}$$

$$u_3 = 0.75\,\exp\left[-\frac{(9x-2)^2+(9y-2)^2)}{4}\right] + 0.75\,\exp\left[-\frac{(9x+1)^2}{49} - \frac{9y+1}{10}\right] + 0.5\,\exp\left[-\frac{(9x-7)^2+(9y-3)^2}{4}\right] - 0.2\,\exp\left[-(9x-4)^2-(9x-7)^2\right]\,, \tag{30}$$

$$u_4 = \frac{25}{25+(x-0.2)^2+2y^2}\,. \tag{31}$$

These problems have been used by several authors to analyze the performance of various RBF type methods [6,7,16,29]. We have also used these problems to analyze the accuracy of the RBF-FD method with a constant optimal shape parameter [2].

Figure 12 shows with bars the infinite norms of the errors using the optimal variable shape parameters c_j^+ for the four problems (28)-(31). In these problems, we have used a regular mesh of 31×31 nodes. Also shown with dashed lines are the infinite norms of the errors with constant values of the shape parameter c.

Table 6
Same as Table 1 but for the Laplacian problem with solutions (28)-(31). In every case, N is equal to 31 31 structured nodes.

Structured nodes							
f	$\min(\mathbf{c}_e^+)$	$\max(\mathbf{c}_e^+)$	$\%N$	$\mathbf{E}(\mathbf{c}_e^+)$	c_e	$\mathbf{E}(c_e)$	$\mathbf{E}$
u_1	1.0387	1.0387	0	1 394 10 ^{6}	1.0387	1 345 10 ^{6}	9 144 10 ^{4}
u_2	0.2566	5.1882	74.1	8 000 10 ^{4}	0.5978	1 043 10 ^{3}	1 868 10 ^{3}
u_3	0.2500	7.8858	17.5	3 032 10 ^{3}	0.4935	1 758 10 ^{3}	4 604 10 ^{3}
u_4	4.1053	6.2108	0	9 405 10 ^{10}	4.4957	7 440 10 ^{8}	9 727 10 ^{7}

In the top left image of Fig. 12 we show the results from problem (28). This is a very peculiar problem because an optimal value of the shape parameter c_j^+ exists for all nodes, and the value of c_j^+ is the same for all of them (notice that the bar for the optimal $\mathbf{c}_e^+$ is just one point). This is because the solution of this problem is an eigenfunction of the Laplacian. Since c_j^+ is independent of the node location x_j, the resulting error can be made as small as needed by just computing the value of $c_j^+ = c$ with su cient accuracy. These results are also summarized in Table 6.

The top right image of Fig. 12 shows the results from problem (29). In this case, there is a very small improvement in accuracy. The reason for this can be explained by considering the results in Table 6. Notice that there is a high percentage of nodes ($\%N = 74\ 1\%$) for which c_j^+ does not exist and, therefore, in which the conventional FD approximation is used with the corresponding deterioration of the overall accuracy.

A similar behavior is observed for problem (30), where the accuracy is worse with the optimal variable shape parameter c_j^+ than with the optimal constant one c (see the bottom left image of Fig. 12).

On the contrary, problem (31) is an example where the use of a variable shape parameter leads to a very signi cant improvement of the accuracy (see the bottom right image of Fig. 12). In fact, the in nite norm of the error with the optimal variable $\mathbf{c}_e^+$ is 9 405 10 ^{10}, nearly two orders of magnitude improvement with respect to the constant optimal value c for which the error is 7 440 10 ^{8}. Again, the reason for this high accuracy is that, in this case, there is an optimal shape parameter c_j^+ for all nodes ($\%N = 0$ in the last row of Table 6).

To overcome the problem of the existence of optimal shape parameters c_j^+ for problems (29) and (30), we have solved them using the RBF (22) in a way analogous to that described in Subsection 5 for convection-di usion problems.

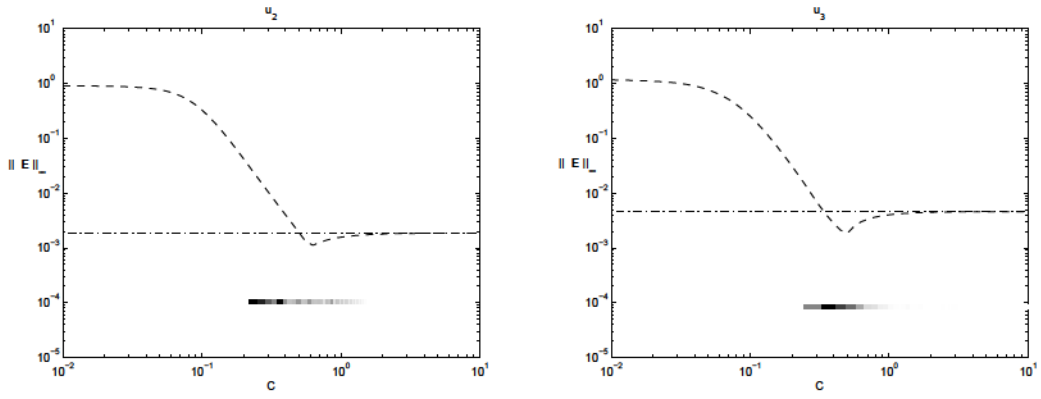

Fig. 13. Infinite norms of the errors from problem (24) with exact solutions (29) and (30) using the generalized multiquadrics (22). As in Fig. 12, we use $N = 31 \times 31$ structured nodes.

The corresponding local RBF-FD error is

$$\epsilon_5(\mathbf{x}_j, c_j, \beta_j) = \frac{h^2}{12}\left(u^{(4,0)}(\mathbf{x}_j) + u^{(0,4)}(\mathbf{x}_j)\right) - \frac{h^2}{c_j^2}\frac{(\beta_j-6)(\beta_j-2)}{2(\beta_j-4)}\left(u^{(2,0)}(\mathbf{x}_j) + u^{(0,2)}(\mathbf{x}_j)\right) + \frac{h^2}{c_j^4}\frac{(\beta_j-8)(\beta_j-2)\beta_j}{2(\beta_j-4)}\,u(\mathbf{x}_j) + O\left(h^3\, P_2(1/c_j^2)\right). \tag{32}$$

The new (node-dependent) parameter β_j^+ in (22) is chosen so that there exists a valid optimal shape parameter $c_j^+ \gg h$ at each node of the grid, as explained in Section 5. Figure 13 shows the results corresponding to problems (29) and (30) using the generalized multiquadric RBF (22) with $c_{min} = 0.2$. In both cases, there is an improvement of two orders of magnitude in the accuracy of the computed solutions.

7 Conclusions

In this follow up paper to our previous work in [2], we present a novel technique to compute the solution of PDEs with the multiquadric based local RBF finite difference method (RBF-FD) using an optimal variable shape parameter c_j at each node of the computational domain. We show that a simple and inexpensive numerical strategy can give rise to several orders more accurate solutions if there exists an optimal value of the shape parameter for most of the grid points of the domain. However, if there are many nodes for which an optimal value of c does not exist, the accuracy was similar to that obtained with an optimal constant c or even with standard FD formulas. For those cases we notice that using generalized multiquadrics as RBF and choosing the exponent β and the shape parameter c appropriately, guarantees the existence

of optimal shape parameter for all the nodes. In this way, we are able to obtain very signi cant improvements in accuracy for all the examples analyzed both with structured and unstructured grids.

We emphasize that to compute the optimal local shape parameter to order $O(h^2)$ it is only necessary to approximate the solution $u(\mathbf{x})$ and certain derivatives to order $O(h^2)$. In practice, this can be achieved by rst computing the standard nite di erence solution, then use this solution to estimate the optimal local shape parameters c_j^+, and nally use these values to compute the optimal RBF-FD solution. For unstructured grids in 2D it is not advisable to estimate derivatives through nite di erence formulas, since this will require the selection of appropriate stencils for each derivative. Instead, one can use the RBF global method on a coarse grid and use this solution to approximate $u(\mathbf{x})$ and the needed derivatives on the unstructured grid.

8 Acknowledgements

This work has been supported by Spanish MICINN grants FIS2010-18473, CSD2010-00011 and by Madrid Autonomous Region grant S2009-1597. M.K. acknowledges Fundacion Caja Madrid for its nancial support.

References

[1] V. Bayona, M. Moscoso, M. Carretero and M. Kindelan, RBF-FD formulas and convergence properties, J. Comput. Phys. 229 (2010) 8281-8295.

[2] V. Bayona, M. Moscoso, M. Kindelan, Optimal constant shape parameter for multiquadric based RBF-FD method, J. Comput. Phys. 230 (2011) 7384-7399.

[3] F. Bernal, M. Kindelan, Use of singularity capturing functions in the solution of problems with discontinuous boundary conditions, Engineering Analysis with Boundary Elements, 33 (2009) 200-208.

[4] G. Chandhini and Y. V. S. S. Sanyasiraju, Local RBF-FD solutions for steady convection-di usion problems, Int. J. Numer. Meth. Engng. 72, (2007) 352-378.

[5] S. Chantasiriwan, Investigation of the use of radial basis functions in local collocation method for solving di usion problems, Int. Comm. in Heat and Mass Transfer, 31 (2004) 1095-1104.

[6] O. Davydov and D. T. Oanh, Adaptive meshless centers and RBF stencils for Poisson equation, J. Comput. Phys. 230, (2011) 287-304.

[7] H. Ding, C. Shu, D. B. Tang, Error estimates of local multiquadric-based di erential quadrature (LMQDQ) method through numerical experiments, Int. J. Numer. Meth. Engng., 63 (2005) 1513-1529.

[8] A. J. M. Ferreira, C. M. C. Roque, G. E. Fasshauer, R. M. N. Jorge, R. C. Batra, Analysis of Functionally Graded Plates by a Robust Meshless Method, Mechanics of Advanced Materials and Structures 14 (2007) 577-587.

[9] A. J. M. Ferreira, G. E. Fasshauer, R. C. Batra, J. Dias Rodrigues, Analysis of natural frequencies of composite plates by an RBF-pseudospectral method, Composite Structures 79 (2007) 202-210.

[10] B. Fornberg, E. Lehto, Stabilization of RBF-generated nite di erence methods for convective PDEs, J. Comput. Phys. 230 (2011) 2270-2285.

[11] J. Halton, On the e ciency of certain quasi-random sequences of points in evaluating multi-dimensional integrals, Numerische Mathematik 2, (1960) 84-90.

[12] R. L. Hardy, Multiquadric equations of topography and other irregular surfaces, J. Geophys. Res. 176 (1971) 1905-1915.

[13] E. J. Kansa, Multiquadrics, a scattered data approximation scheme with applications to computational uid dynamics. I. Surface approximations and partial derivatives estimates, Comput. Math. Appl. 19 (1990) 127-145.

[14] E. J. Kansa, Multiquadrics, a scattered data approximation scheme with applications to computational uid dynamics. II. Solutions to parabolic, hyperbolic and elliptic partial di erential equations, Comput. Math. Appl. 19 (1990) 147-161.

[15] S. Kirkpatrick, C. D. Gelatt, M. P. Vecchi, Optimization by Simulated Annealing. Science. New Series 220 (1983) 671-680.

[16] E. Larsson, B. Fornberg, A numerical study of some Radial Basis Function based Solution Methods for Elliptic PDEs, Comput. Math. Appl. 46 (2003) 891-902.

[17] C. Lee, X. Liu, S. Fan, Local multiquadric approximation for solving boundary value problems, Comp. Mech. 30 (2003) 396-409.

[18] C. M. C. Roque, D. Cunha, C. Shu, A. J. M. Ferreira, A local radial basis functions-Finite di erences technique for the analysis of composite plates, Engineering Analysis with Boundary Elements 35 (2011) 363-374.

[19] Y. V. S. S. Sanyasiraju, G. Chandhini, Local radial basis function based gridfree scheme for unsteady incompressible viscous ows, J. Comput. Phys. 227 (2008) 8922-8948.

[20] B. Sarler, R. Vertnik, Meshfree explicit local radial basis function collocation method for di usion problems, Comput. Math. Appl. 51 (2006) 1260-1282.

[21] B. Seibold, M-Matrices in meshless nite di erence methods, PhD thesis, Department of Mathematics, University of Kaiserslautern, Shaker-Verlag (2006).

[22] B. Seibold, Minimal positive stencils in meshfree nite di erence methods for the Poisson equation, Comput. Methods Appl. Mech. Engrg. 198 (2008) 592-601.

[23] Y. Y. Shan, C. Shu and N. Qin, Multiquadric Finite Di erence (MQ-FD) Method and its Application, Adv. Appl. Math. Mech., 1 (2009) 615-638.

[24] C. Shu, H. Ding, K.S. Yeo, Local radial basis function-based di erential quadrature method and its application to solve two-dimensional incompressible Navier-Stokes equations, Computer Methods in Applied Mechanics and Engineering, 192, 3, (2003) 941-954.

[25] D. Stevens, H. Power, M. Leesa, H. Morvan, The use of PDE centres in the local RBF Hermitian method for 3D convective-di usion problems, J. Comput. Phys. 228 (2009) 4606-4624.

[26] A. I. Tolstykh and D. A. Shirobokov, On using radial basis functions in a nite di erence mode with applications to elasticity problems, Computational Mechanics 33, (2003) 68-79.

[27] J. G. Wang, G. R. Liu, A point interpolation meshless method based on radial basis functions, Int. J. Numer. Meth. Engng., 54 (2002) 1623-1648.

[28] G. B. Wright, Radial basis function interpolation: numerical and analytical developments, Ph.D. thesis, University of Colorado, Boulder (2003).

[29] G. B. Wright, B. Fornberg, Scattered node compact nite di erence-type formulas generated from radial basis functions, J. Comput. Phys. 212, (2006) 99-123.